Comprehensive analysis of the $A-X$ spectrum of I_2: An application of near-dissociation theory

D. R. T. Appadoo, R. J. Le Roy, and P. F. Bernath
Guelph-Waterloo Centre for Graduate Work in Chemistry, University of Waterloo, Waterloo, Ontario N2L 3G1, Canada

S. Gerstenkorn, P. Luc, J. Vergès, J. Sinzelle, J. Chevillard, and Y. D'Aignaux
Laboratoire Aimé Cotton, Centre National de la Recherche Scientifique, Bâtiment 505, Université de Paris-Sud, 91405 Orsay Cedex, France

(Received 3 May 1995; accepted 9 October 1995)

High resolution absorption spectra of the $A\ ^3\Pi_{1u}-X\ ^1\Sigma_g^+$ system of I_2, consisting of some 9552 lines of some 79 bands spanning the vibrational range $v'=0-35$ and $v''=3-17$, have been recorded and analyzed. A fit to them which uses the previously determined accurate molecular constants for the $X\ ^1\Sigma_g^+$ state yields an accurate new set of molecular constants for the A state, including the Λ doubling constants. The A-state vibrational and inertial rotational constants, as well as mechanically consistent centrifugal distortion constants, are represented by near-dissociation expansions, yielding an accurate representation of the experimental data which also provides a reliable global representation of *all* observed and unobserved vibration–rotation levels of this state. © *1996 American Institute of Physics.* [S0021-9606(96)00203-1]

I. INTRODUCTION

Iodine is one of the most widely studied halogen molecules, and its high resolution near infrared/visible absorption spectrum is widely used as a spectroscopic wavelength standard. Transitions involving the ground $X\ ^1\Sigma_g^+$ state and the four low-lying excited states, $A'\ ^3\Pi_{2u}$, $A\ ^3\Pi_{1u}$, $^1\Pi_{1u}$, and $B\ ^3\Pi_{0u}^+$, lie in the near infrared/visible region of the spectrum.[1–3] The potential curves for these states[4–6] are illustrated in Fig. 1. Due to the repulsive nature of the $^1\Pi_{1u}$ potential, the $^1\Pi_{1u}-X\ ^1\Sigma_g^+$ spectrum consists of a broad continuum. Moreover, transitions between the A' and X states are forbidden because they would have $\Delta\Omega=2$. However, the A' state has been accessed indirectly by utilizing the high-lying D' ion-pair state, and its potential curve is known.[5,7–10] Although not directly involved in the absorption spectrum, this state may be a source of perturbations for the stronger allowed transitions.

The $B-X$ spectrum is the most intense of the allowed electronic transitions, and it provides the principal contribution to the visible absorption spectrum of iodine vapor. Extensive studies of this system have yielded accurate molecular constants and potential energy curves for both the X and B states. In particular, workers at the Laboratoire Aimé Cotton have published a comprehensive *Iodine Atlas* spanning the infrared and visible region between 7 220 and 20 000 cm^{-1} that is widely used as a wavelength standard.[11–16] As part of that work, Gerstenkorn and Luc analyzed the $B-X$ spectrum and reported accurate spectroscopic constants describing the properties of X-state vibrational levels ranging from $v''=0$ to 19, and B-state levels from $v'=0$ to 80.[4]

Other groups have studied the higher vibrational levels of the X state. In 1960, Verma observed ultraviolet fluorescence emission into the ground state and reported spectroscopic constants for levels spanning the region from $v''=0$ to 84.[17] Ten years later, a reanalysis of his data together with the green-line resonance series observed by Rank and Baldwin[18,19] yielded a more accurate set of X-state spectroscopic constants.[20] Then in 1986, Martin *et al.*[21] recorded the laser induced fluorescence of the $B-X$ system using Fourier transform techniques, and were able to probe the X state all the way to $v''=107$. However, they did not observe any transitions involving the first eight vibrational level of the ground state. Thus the most accurate molecular constants for the lower portion of the X state remain those obtained by Gerstenkorn and Luc from the $B-X$ absorption spectra.[4]

The $A-X$ spectrum lies in the near infrared region, is relatively weak, and is obscured by the strong $B-X$ spectrum at shorter wavelengths. These factors have hindered the study of this system, so the lowest optically accessible excited state of iodine is relatively poorly known. The first direct observation of this system was Brown's 1931 absorption measurement of four series of band heads, spanning a range of 22 vibrational levels.[22] However, he was unable to determine an absolute A-state vibrational numbering. Four decades later, Tellinghuisen's analysis of the I_2 visible continuum indicated that the A-state potential well had to be distinctly deeper than Brown's data had suggested.[6] In the first study of the $A-X$ system at rotational resolution, Ashby confirmed this conclusion and showed that Brown's provisional v' numbering should be increased by at least twelve units.[23] Shortly afterwards, Ashby and Johnson[24] and Gerstenkorn *et al.*[25] independently concluded that this new v' numbering should be increased by an additional two units, yielding vibrational assignments which now appears to be conclusive.[26] In 1981, Viswanathan *et al.*[27] reported some new band head measurements for $v(A)=0-8$ together with a detailed analysis of all data available at that time. However, their extended range and much higher resolution means that the Fourier transform measurements of Ref. 15 supplant all of the earlier results.

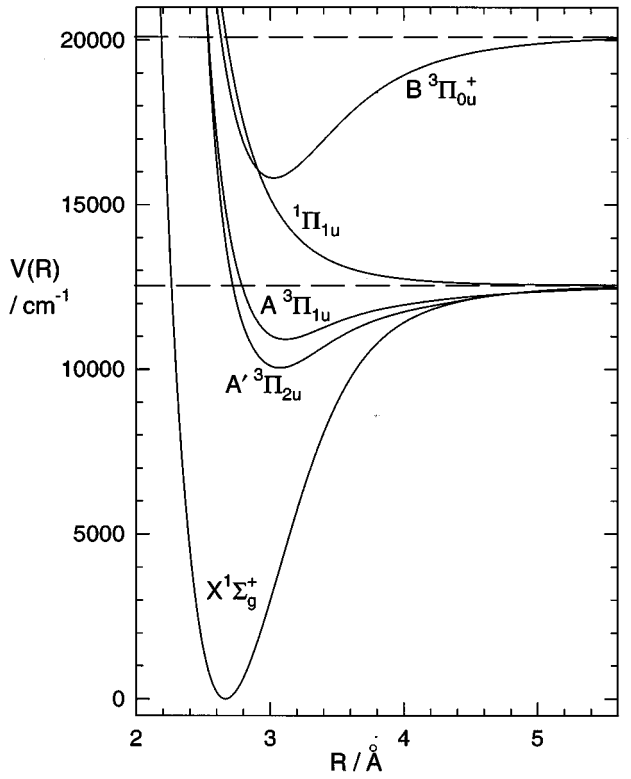

FIG. 1. Potential energy curves for the X, A', A, $^1\Pi_{1u}$, and B electronic states of I_2.

The conclusions of Gerstenkorn *et al.*[25] regarding the vibrational assignments were based on the high resolution Fourier transform spectra which comprise the infrared portion of the *Iodine Atlas*.[15] However, while they reported preliminary molecular constants for the $v'=0$ level, no new overall description of the A state has yet been extracted from those data. The present paper addresses this problem by reporting the assignment of many new bands of the $A-X$ system recorded by Gerstenkorn *et al.*[15,25] This more complete data set has been fitted to both Dunham and near-dissociation expansions to yield a comprehensive and accurate set of molecular constants describing the $A\ ^3\Pi_{1u}$ state of I_2 all the way to dissociation.

II. EXPERIMENT

An absorption cell 1.5 m in length was filled with iodine gas and placed in an oven which was heated to 800 K. A side arm of the cell was kept at a temperature between 333 and 353 K in order to prevent the iodine pressure in the cell from becoming too high. The cell was then coupled to the Fourier transform spectrometer, which is described in detail in Ref. 28. For this experiment, the background continuum was provided by a tungsten iodide quartz lamp. The experimental conditions are summarized in Table I.[15]

The absorption spectrum of iodine was recorded from 7 200 to 11 200 cm^{-1} and the results published in the form of an Atlas.[15] The spectrum in this region consists of approximately 16 450 lines, whose positions were measured with a typical accuracy of ± 0.005 cm^{-1}. In the present work, 9552 of these transition frequencies were arranged into series using the interactive color spectral assignment program ''Loomis–Wood,'' written by Jarman. The series were assigned to some 79 bands spanning the vibrational ranges $v''=3$–17 and $v'=0$–35, which are distributed as shown in Table II. Heating the absorption cell to 800 K allowed transitions involving rotational levels as high as $J=200$ to be observed for some vibrational levels. For each v' level, the range of rotational levels spanned by this data set is indicated by the shaded region in Fig. 2.

While Q branches were observed for all of the observed bands, the lower intensities of P and R branch transitions made them much more difficult to locate, and they were only measured for 21 bands. However, this was sufficient to unambiguously confirm the v'' vibrational assignments by pro-

TABLE II. Ranges of A state v' levels for $A-X$ bands of I_2 assigned and fitted in the present analysis.

	v' range	
v''	Q branch	P & R branches
3	23–35	
4	10–21, 23–35	13–16, 23, 26–28, 30–32
5	10–24	11–13, 15–17
6	10, 11, 22, 23	
7	9, 10	9
8	8, 9	8
9	7–9	7–9
10	6, 7	
11	5, 6	
12	4, 5	
13	3, 4	
14	2, 3	
15	1, 2	
16	0, 1	
17	0	

TABLE I. Summary of experimental conditions: T_1 is the cell temperature, T_2 the side arm temperature, P the iodine pressure, and ρ the signal-to-noise ratio (Ref. 15).

Spectra	Range (cm^{-1})	T_1 (K)	T_2 (K)	P (Torr)	ρ
A	7200–7600	773	353	15	1.5
	7500–9500	773	353	15	3
B	9000–9500	623	333	5	3
	9500–9800	623	333	5	5
	9700–11 200	623	333	5	7

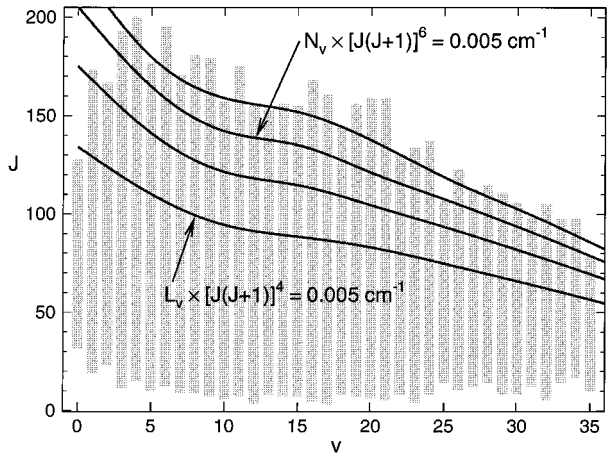

FIG. 2. The shaded region indicates the J ranges associated with the present data set, while the curves indicate the values of J at which the term value contributions of the calculated centrifugal distortion constants for $m=4-7$ equal the experimental uncertainty.

viding independent estimates of the B_v'' values for comparison with those predicted by the molecular constants of Ref. 4.

III. ANALYSIS

A. Purely empirical fits

Since P and R branches were not obtained for substantial segments of the v' range (see Table II), it was impossible to determine reliable independent upper and lower state rotational constants for these bands. Fortunately, Gerstenkorn and Luc have reported molecular constants which accurately describe the ground electronic state over the complete range spanned by the present data set.[4] Thus in all of the present fits, the ground-state rovibrational energies were represented by the conventional double Dunham expansion

$$E_X(v'',J'') = \sum_{l,m} Y''_{l,m}(v''+\tfrac{1}{2})^l [J''(J''+1)]^m, \tag{1}$$

with the $\{Y''_{l,m}\}$ parameters held fixed at the values reported in Ref. 4.

For the $A\ ^3\Pi_{1u}$ state, it is convenient to first write the rovibrational energies in the form

$$E_A^{e,f}(v,J) = \sum_{m=0}^{m_{\max}} K_m(v)[J(J+1)-1]^m \pm \sum_{l,m} Q_{l,m}(v+\tfrac{1}{2})^l [J(J+1)-1]^m, \tag{2}$$

where $K_0(v)$ represents the pure vibrational energy, $K_1(v)$ the inertial rotational constant B_v, and $K_m(v)$ for $m \geqslant 2$ the usual centrifugal distortion constants.[29] The second sum in Eq. (2) is a simple empirical representation of the Λ-doubling energy associated with states of nonzero orbital angular momentum, with the parity superscript labels e and f corresponding, respectively, to the $+$ and $-$ sign preceding this sum. As usual, the $\Omega=1$ value appearing in the rotational expansion variable $[J(J+1)-\Omega^2]$ represents the projection of the total electronic angular momentum on the internuclear axis of the molecule for this state.

As the first stage of the present analysis, the fits to the assigned transition frequencies of the $A-X$ system,

$$\nu^{e,f}(v',J';v'',J'') = E_A^{e,f}(v',J') - E_X(v'',J''), \tag{3}$$

used a conventional Dunham expansion in $(v+\frac{1}{2})$ to represent each of the expansion coefficients of Eq. (2)

$$K_m(v) = \sum_{l=0}^{l_{\max}(m)} Y'_{l,m}(v+\tfrac{1}{2})^l. \tag{4}$$

A wide range of Dunham models were tested with respect to the criteria of compactness and accuracy, and the most satisfactory fit was obtained with one for which $m_{\max}=4$ (corresponding to the use of B_v, D_v, H_v, and L_v rotational constants) and the set of polynomial orders were $l_{\max}(m)=12$, 13, 9, 4, and 2, for $m=0$ to 4, respectively. While further work (see below) showed that the data are sensitive to yet higher-order ($m>4$) distortion constants, in unconstrained fits the high degree of interparameter correlation prevented their empirical determination. For the Λ-doubling energy, the associated expansion required only a two-term $m=1$ sum with $l_{\max}(1)=1$.

The empirical Dunham and Λ-doubling expansion parameters yielded by this fit are reported in Table III. The number of significant digits listed for each parameter was defined using the Watson criterion[30] which requires that on average the net effect of the rounding on predictions of each input datum be less than 0.1 times the standard error of the fit. These expansions reproduce the observed transitions reasonably well, yielding a dimensionless standard deviation of $\overline{\sigma}=1.33$ (corresponding to a standard error of ca. 0.0066 cm^{-1}). However, the empirical centrifugal distortion constants obtained in this way are not entirely satisfactory.

B. Fits with constrained centrifugal distortion constants

It has long been known that centrifugal distortion constants (CDC's) of a diatomic molecule are not independent physical parameters, but can be calculated from a knowledge of the potential energy curve, and hence are implicitly determined by a knowledge of the vibrational energies $G(v)$ and inertial rotational constants B_v.[31–36] Moreover, CDC's determined empirically from fits to experimental data are actually "effective" constants which contain errors due to experimental uncertainties, interparameter correlation, and the effects of neglecting undetermined higher-order CDC's, as well as contributions from local perturbations. As a result, these effective empirical CDC's may differ significantly from "mechanical" values determined by the potential curve defined by the associated $G(v)$ and B_v expressions. This limits both their physical significance and their utility in making predictions for unobserved higher-J levels. It also introduces com-

TABLE III. Empirical Dunham constants for the A state of I_2 (in cm^{-1}, with 95% confidence limit uncertainties in parentheses) obtained from a linear least squares fit to Eqs. (2)–(4) which yielded a dimensionless standard error of $\bar{\sigma}=1.33$. The T_e value neglects $Y_{0,0}$ for both states.

	$m=0$		$m=1$		$m=2$		$m=3$		$m=4$	
T_e	10907.4159	(0.0088)								
$Y_{0,m}$			2.739 831 8$\times10^{-2}$	(2.0$\times10^{-6}$)	$-1.010\,998\times10^{-8}$	(1.8$\times10^{-10}$)	-2.497×10^{-15}	(7.2 $\times10^{-15}$)	$-6.578\,2\times10^{-19}$	(1.1 $\times10^{-19}$)
$Y_{1,m}$	92.946 344 4	(0.016)	$-2.746\,886\times10^{-4}$	(2.4 $\times10^{-6}$)	$2.397\,22\times10^{-10}$	(1.2 $\times10^{-10}$)	$8.482\,1\times10^{-15}$	(1.9 $\times10^{-15}$)	$1.607\,4\times10^{-19}$	(2.6 $\times10^{-20}$)
$Y_{2,m}$	$-1.565\,036\,75$	(0.012)	$-8.828\,421\times10^{-6}$	(1.7 $\times10^{-6}$)	$-7.463\,508\times10^{-10}$	(5.3 $\times10^{-11}$)	$-4.082\,31\times10^{-15}$	(1.8 $\times10^{-16}$)	$-2.156\,66\times10^{-20}$	(1.2 $\times10^{-21}$)
$Y_{3,m}$	2.894 001 7$\times10^{-2}$	(4.6$\times10^{-3}$)	3.850 381 9 $\times10^{-6}$	(6.8 $\times10^{-7}$)	$2.369\,975\,8\times10^{-10}$	(1.2 $\times10^{-11}$)	$3.139\,13\times10^{-16}$	(9.2 $\times10^{-18}$)		
$Y_{4,m}$	$-1.251\,274\,502\times10^{-2}$	(1.0$\times10^{-3}$)	$-1.900\,324\,819\times10^{-6}$	(1.7 $\times10^{-7}$)	$-3.930\,564\,52\times10^{-11}$	(1.6 $\times10^{-12}$)	$-7.169\,16\times10^{-18}$	(1.8 $\times10^{-19}$)		
$Y_{5,m}$	2.192 826 393$\times10^{-3}$	(1.4$\times10^{-4}$)	4.485 302 543 $\times10^{-7}$	(2.8 $\times10^{-8}$)	$3.485\,565\,35\times10^{-12}$	(1.3 $\times10^{-13}$)				
$Y_{6,m}$	$-2.489\,494\,709\,7\times10^{-4}$	(1.3$\times10^{-5}$)	$-6.310\,367\,966\,2\times10^{-8}$	(3.1 $\times10^{-9}$)	$-1.752\,989\,421\times10^{-13}$	(6.1 $\times10^{-15}$)				
$Y_{7,m}$	1.878 268 835 4$\times10^{-5}$	(8.3$\times10^{-7}$)	5.706 353 133 0 $\times10^{-9}$	(2.4 $\times10^{-10}$)	$5.038\,662\,59\times10^{-15}$	(1.8 $\times10^{-16}$)				
$Y_{8,m}$	$-9.200\,259\,398\,5\times10^{-7}$	(3.5$\times10^{-8}$)	$-3.430\,075\,991\,39\times10^{-10}$	(1.3 $\times10^{-11}$)	$-7.729\,567\,6\times10^{-17}$	(2.8 $\times10^{-18}$)				
$Y_{9,m}$	2.883 255 490 38$\times10^{-8}$	(1.0$\times10^{-9}$)	1.386 972 111 88 $\times10^{-11}$	(4.8 $\times10^{-13}$)	$4.911\,795\,9\times10^{-19}$	(1.8 $\times10^{-20}$)				
$Y_{10,m}$	$-5.586\,491\,773\,8\times10^{-10}$	(1.8$\times10^{-11}$)	$-3.734\,906\,526\,09\times10^{-13}$	(1.2 $\times10^{-14}$)						
$Y_{11,m}$	6.107 080 936 0$\times10^{-12}$	(2.0$\times10^{-13}$)	6.430 434 346 9 $\times10^{-15}$	(2.1 $\times10^{-16}$)						
$Y_{12,m}$	$-2.885\,455\,276\times10^{-14}$	(9.1$\times10^{-16}$)	$-6.410\,284\,755\,9\times10^{-17}$	(2.1 $\times10^{-18}$)						
$Y_{13,m}$			2.816 284 289 $\times10^{-19}$	(9.3 $\times10^{-21}$)						
$Q_{0,1}$			1.72 $\times10^{-7}$	(1.1 $\times10^{-7}$)						
$Q_{1,1}$			1.941 $\times10^{-7}$	(5.7 $\times10^{-9}$)						

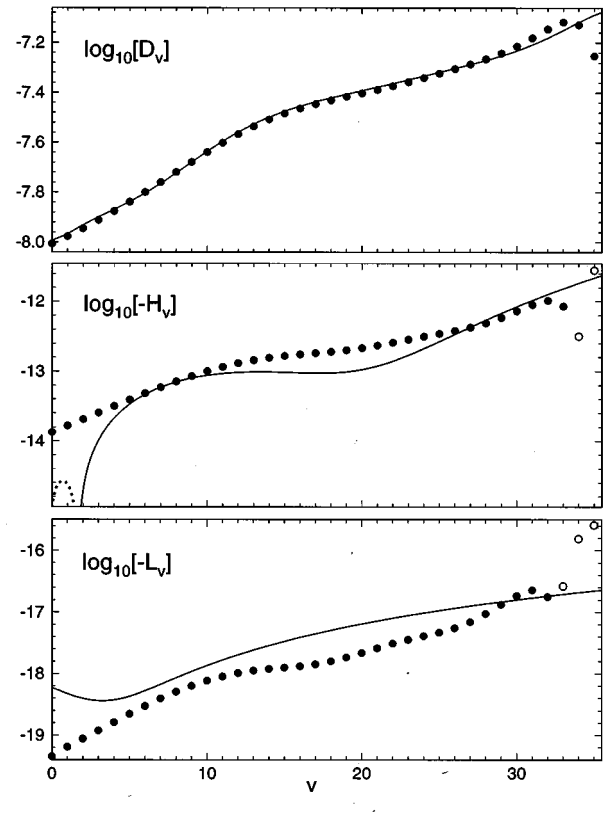

FIG. 3. Comparison of the empirical Dunham expansions of Table III for the centrifugal distortion constants of A state I_2 (curves), with numerically calculated values (symbols) obtained after three cycles of an iterative constrained analysis. The dotted curves and open symbols represent situations where these quantities have changed sign and taken on positive values (see the text).

pensating errors into the associated empirical $G(v)$ and B_v expressions, and hence into the potential energy function obtained from them.

In the present case this problem is illustrated by Fig. 3, which compares our empirical Dunham polynomials for the A-state centrifugal distortion constants (curves) with "mechanically consistent" values (symbols) calculated from the A-state potential curve determined from Dunham $G(v)$ and B_v expansions yielded by the constrained fit (see below). While the agreement is fairly good for the leading distortion constant $K_2(v)=-D_v$, the empirical Dunham polynomial expressions for the higher-order ($m\geqslant3$) terms have substantially larger errors, and that for $K_3(v)=H_v$ even undergoes a spurious sign change at small v (indicated by the dotted curve segment).

In order to obtain a set of molecular constants which provide reliable predictions for rotational levels well beyond the range of the input data, it is clearly essential to require that the centrifugal distortion constants [$K_m(v)$'s for $m\geqslant2$] be mechanically consistent with the vibrational energies $G(v)$ and inertial rotational constants B_v (i.e., with $K_0(v)$ and $K_1(v)$). One means of achieving this consistency is to fix the distortion constants at values calculated from the best current estimate of the potential, when fitting the experimental data to determine the desired $G(v)$ and B_v

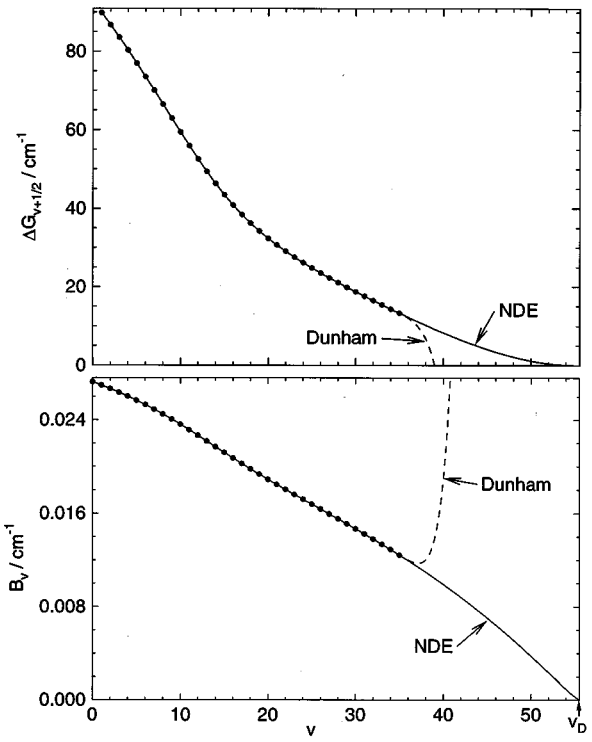

FIG. 4. For the vibrational spacings $\Delta G_{v+1/2}$ and inertial rotational constants B_v of A state I_2, comparison of the extrapolation behavior of the Dunham expansions of Table III (dashed curves) with the near-dissociation expansions of Table V (solid curves) beyond the range of the experimental data (points).

expressions.[35,37–39] This approach may be initiated by first using the unconstrained polynomial fit to Eqs. (2)–(4) to provide preliminary estimates of the A-state $G(v)$ and B_v functions (together with empirical effective distortion constant expansions). The potential energy curve obtained by applying the RKR inversion procedure to these expressions may then be used to generate numerical values of all relevant CDC's. A new fit to the experimental data in which the distortion constants are held fixed at these calculated values then yields improved $G(v)$ and B_v expressions, which in turn yield an improved potential curve, and improved estimates of the CDC's. This procedure is iterated until convergence is achieved. In the present work, the RKR inversion procedure was performed using a computer program based on the method of Tellinghuisen,[40–43] while the centrifugal distortion constants $(D_v, H_v, \ldots, N_v)$ were calculated using a program based on Tellinghuisen's implementation of the method of Hutson.[36,42–45]

Unfortunately, some difficulties are encountered on applying the constrained self-consistent fitting procedure described above when the $G(v)$ and B_v functions are represented by the conventional polynomial expansions of Eq. (4). In particular, with successive iterations the numerically calculated distortion constants tended to behave increasingly irregularly for vibrational levels near the upper end of the range for which data are available. This is illustrated in Fig. 3 by the irregular behavior of the calculated values (points) for levels approaching $v'=35$; note that the hollow symbols there represent calculated values that have actually changed sign and become positive; these results were obtained after three cycles of the iterative procedure described above. The irregularities in Fig. 3 can be attributed to slightly unphysical behavior of the calculated RKR turning points at the end of the range, and the unreliability of extrapolation beyond them. This in turn is due to the well-known unreliable extrapolation properties of high-order Dunham polynomials. The latter problem is clearly illustrated by the dashed curves in Fig. 4, which show the behavior of the empirical Dunham expansions (for $m=0$ and 1) of Eq. (4) and Table III. While apparently well-behaved up to the last observed level, $v'=35$, the vibrational spacings $\Delta G_{v+1/2}$ implied by the empirical twelfth-order Dunham polynomial of Table III drop off sharply immediately past this point, while the associated 13th-order B_v polynomial abruptly goes through a minimum and increases rapidly. To remove this unreasonable behavior and to allow proper convergence of the constrained self-consistent fitting procedure, better-behaved representations of the $G(v)$ and B_v functions are clearly required.

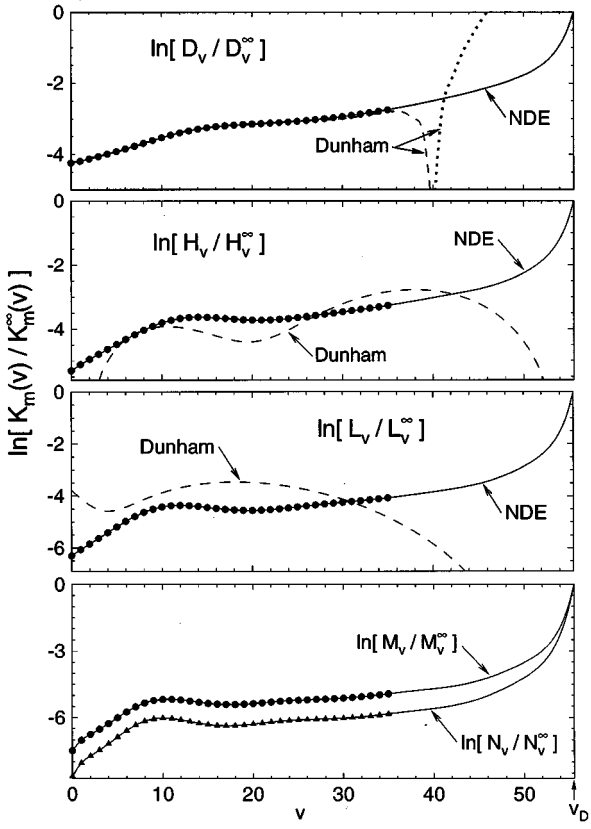

FIG. 5. After scaling by the limiting near-dissociation theory term $K_m^\infty(v)$, comparison of the converged self-consistent calculated CDC's over the range of the experimental data (points) with the present recommended near-dissociation expansions for them (solid curves), and with the empirical Dunham expansions of Table III (dashed and dotted curves). The dotted curve segment for D_v indicates that the empirical Dunham expansion has changed sign and taken on negative values.

C. Constrained fits based on near-dissociation expansions

"Near-dissociation expansions" (NDE's) are expressions for vibrational energies, B_v constants and other vibrational-quantum-number dependent molecular properties which incorporate the theoretically known limiting near-dissociation behavior of that property into an empirical expansion determined from a fit to data. In addition to being able to compactly and accurately represent large bodies of experimental data,[39] these expansions tend to be well behaved in the neighborhood of the highest observed levels, and they are inherently much more reliable in extrapolations to predict the properties of unobserved higher vibrational levels.[46–49] In the rest of the present work, the simple Dunham expansions of Eq. (4) are replaced by near-dissociation expansions for most properties of $A\ ^3\Pi_{1u}$ state I_2. The only exception is the A-state Λ-doubling energy, which is always represented by the same empirical two-term Dunham-type expansion used above. $\pm[Q_{0,1}+Q_{1,1}(v+\frac{1}{2})][J(J+1)-1]$.

In the present analysis, the near-dissociation expansions used for the vibrational energies have the form

$$K_0(v)=D-K_0^{\infty}(v)[L/M], \tag{5}$$

where D is the dissociation energy, $[L/M]$ are the rational polynomials

$$[L/M]=\frac{1+\Sigma_{i=1}^{L}p_{t+i}(v_D-v)^{t+i}}{1+\Sigma_{j=1}^{M}q_{t+j}(v_D-v)^{t+j}}, \tag{6}$$

and the fixed power $t=1$ is determined by the theory of deviations from limiting near-dissociation behavior.[50,51] The analogous expressions for the rotational and centrifugal distortion constants are

$$K_m(v)=K_m^{\infty}(v)\exp\left(\sum_{i=1}p_i^m(v_D-v)^i\right). \tag{7}$$

In both of these functions, the term

$$K_m^{\infty}(v)=X_m(n,C_n)(v_D-v)^{[2n/(n-2)]-2m}, \tag{8}$$

introduces the theoretically known limiting near-dissociation behavior of that property,[46–48,52–54] where v_D is the (usually noninteger) effective vibrational index at dissociation, and n and $X_m(n,C_n)$ are known constants determined by the nature of the asymptotic long-range behavior of the potential

$$V(R)=D-C_n/R^n. \tag{9}$$

As for most electronic states of I_2, theory shows that $n=5$ for the long-range potential of the $A\ ^3\Pi_{1u}$ state.[55,56] The value of $C_5=59\,500\ \mathrm{cm^{-1}}\ \text{Å}^5$ was taken from Ref. 57; this yields the (rounded) constants $X_m(5,C_5)=5.96\times10^{-3}$, 7.66×10^{-4}, -9.99×10^{-6}, -1.15×10^{-7}, -3.47×10^{-9}, -1.41×10^{-10}, and $-6.68\times10^{-12}\ \mathrm{cm^{-1}}$ for $m=0$–6, respectively.

After testing a variety of NDE models against the usual criteria of accuracy and compactness, it was concluded that an optimal combination consisted of an $[L/M]=[8/2]$ rational polynomial representation for the $G(v)$ function and a 12th-order exponent polynomial for the B_v function (note that the expansions of Eq. (7) start with the linear term). In addition to the parameters in these expansions, the effective vibrational index at dissociation v_D was varied in the fits. However, the energy of the dissociation limit $D=D_0=12\,440.243\ \mathrm{cm^{-1}}$ was held fixed at the value determined from the (much shorter) B-state vibrational extrapolation.[58] The solid curves in Fig. 4 illustrate the plausible and mutually consistent manner in which the resulting NDE functions for these properties approach dissociation. Moreover, the points shown in Fig. 5 demonstrate that even after several cycles of constrained fits (see Sec. III E), the calculated distortion constants based on potentials defined by these near-dissociation expansions show none of the irregular behavior near $v'=35$ seen in Fig. 3.

TABLE IV. Dimensionless standard errors $\overline{\sigma}$ of various global fits performed using Dunham and near-dissociation expansion representations for $G(v)$ and B_v, and a variety of representations of the centrifugal distortion constants. In all cases, the Dunham and NDE expansions have the orders and form indicated in the text.

		Fits with constrained CDC's		
			Near-dissociation expansions	
$m_{\max}$	Unconstrained empirical Dunham fit[a]	Dunham $K_{\max}=K_{\max}^{\mathrm{calc}}$	$K_{\max}=K_{\max}^{\mathrm{calc}}$	$K_{\max}$ from Eq. (10)
4	1.33		5.33	2.13
5		10.61	2.41	1.55
6		10.99	1.62	1.40
7				1.38

[a]As per Sec. III A and Table III.

D. Convergence of the expansion in $[J(J+1)-\Omega^2]$

In any fit to experimental data, a question which must always be addressed is how many terms to include in the the rotational energy expansion in powers of $[J(J+1)-\Omega^2]$. For the present case the situation is illustrated by the solid curves in Fig. 2, which indicate the values of J at which the term value contributions of the calculated centrifugal distortion constants for $m=4$–7 equal the experimental uncertainty. They indicate that within a "mechanically consistent" treatment, terms up to at least $m=7$ should be included in the rotational expansion describing the present data for A-state I_2.

In the empirical fits of Sec. III A, ambiguities due to interparameter correlation and the small magnitudes of the higher-order CDC's made it necessary in practice to truncate this expansion at $m=m_{\max}=4$ (the L_v term). This clearly limits the utility of those results for extrapolating to higher J. However, the question of when to truncate the rotational expansion is also a problem in the constrained fits, since there is a practical limit to the order of the distortion constants which may be readily and reliably computed.

In their analysis of the large data set for the $B-X$ absorption spectrum of I_2, Hutson *et al.*[38] (and later Tromp and Le Roy[39]) addressed this problem by simply assuming that the effect of all missing higher-order terms could be taken into account by an empirical scaling of the highest-order directly calculated distortion constants [$M_v=K_5(v)$ in their

TABLE V. Fitted parameters defining the present recommended NDE expressions for the vibrational energies and inertial constants, and Dunham expansion for the Λ-doubling energies for the A state of I_2. The dissociation energy D, the $X_m=X_m(5,C_5)$ constants and the Λ-doubling parameters $Q_{l,1}$ are in cm^{-1}, while all others are dimensionless. The associated fit has a dimensionless standard error of $\overline{\sigma}=1.38$.

Vibrational expansion parameters		Rotational expansion parameters	
X_0	5.96×10^{-3}	X_1	7.66×10^{-4}
$D=D_0(X)$	12 440.243	p_1^1	0.303 801 149
v_D	55.570 ($\pm$0.01)	p_2^1	$-9.349\,498\,161\times10^{-2}$
p_2	$-4.805\,154\,945\times10^{-3}$	p_3^1	$7.945\,002\,009\times10^{-3}$
p_3	$3.486\,659\,935\,1\times10^{-4}$	p_4^1	$-1.214\,824\,009\,6\times10^{-4}$
p_4	$-1.562\,209\,978\,30\times10^{-5}$	p_5^1	$-2.697\,656\,647\,93\times10^{-5}$
p_5	$4.879\,608\,144\,9\times10^{-7}$	p_6^1	$2.433\,128\,549\,164\times10^{-6}$
p_6	$-1.019\,345\,855\,90\times10^{-8}$	p_7^1	$-1.062\,533\,452\,495\times10^{-7}$
p_7	$1.336\,469\,744\,30\times10^{-10}$	p_8^1	$2.845\,324\,630\,715\times10^{-9}$
p_8	$-9.852\,246\,572\times10^{-13}$	p_9^1	$-4.888\,878\,228\,981\times10^{-11}$
p_9	$3.101\,877\,058\times10^{-15}$	p_{10}^1	$5.277\,791\,864\,55\times10^{-13}$
q_2	$-1.311\,907\,393\times10^{-3}$	p_{11}^1	$-3.269\,066\,495\,14\times10^{-15}$
q_3	$2.079\,231\,26\times10^{-5}$	p_{12}^1	$8.878\,720\,269\,4\times10^{-18}$
		k_7	4.04×10^{-2}
		$Q_{0,1}$	7.2×10^{-8}
		$Q_{1,1}$	2.001×10^{-7}

work]. However, the magnitudes of the resulting scaling factors[38,39] (2.6 and 2.38) seem somewhat large. Moreover, it seems questionable that the effect of missing high-order centrifugal terms would be optimally accounted for by a correction term of lower order in $[J(J+1)-\Omega^2]$ which had the same v dependence as that lower order term. A more natural way of accounting for missing higher-order distortion constants is therefore introduced here.

The present approach is suggested by the form of Eq. (8), which shows that the power $\{[2n/(n-2)]-2m\}$ is virtually always negative for high-order centrifugal distortion constants. As a result, $K_m(v)$ values for large m will tend to be most important at high v, where their functional behavior is qualitatively related to that for the next lower-order constant $K_{m-1}(v)$ by the simple factor $(v_D-v)^{-2}$. Thus if reliable directly calculated distortion constants are only available for orders up to $[m_{\max}-1]$, it seems reasonable to represent the effect of yet higher-order constants by the empirical term

$$K_{m_{\max}}(v)=k_{m_{\max}}K^{\mathrm{calc}}_{m_{\max}-1}(v)/(v_D-v)^2, \tag{10}$$

where $k_{m_{\max}}$ is an empirical scaling parameter to be determined in the fit to the experimental data, and $K^{\mathrm{calc}}_{m_{\max}-1}(v)$ are the highest-order directly calculated distortion constants. Further justification for this approximation is provided by the similarity in the shapes of the plots of calculated distortion constants seen in Fig. 5, especially for large m.

For several values of $m_{\max}$, constrained mechanically consistent fits were performed using NDE functions for the vibrational energies and inertial rotation constants, together with calculated values for centrifugal distortion constants, both with and without use of this empirical approximation for missing higher-order CDC's. They show that an $m_{\max}=7$ expansion with the $m\leqslant6$ distortion constants being directly calculated and the $K_7(v)$ constants approximated by Eq. (10) gives an optimum representation of the experimental data. The overall quality of this fit is only marginally different from those those for the analogous $m_{\max}=6$ expansion or the empirical Dunham expansions of Eqs. (2)–(4). However, the present $m_{\max}=7$ NDE-based approach yields a stable and mechanically consistent set of constants which should provide the most reliable predictions for very high J values.

E. Global NDE representation for $A\ ^3\Pi_{1u}$ state of I_2

Our analysis to this point yields NDE representations of the vibrational energies and B_v values for all levels of the A state, together with a tabulation of distortion constants of order up to seven. However, such a tabulation is an inconvenient way in which to summarize and store our knowledge of these distortion constants, or to use them to predict energies of unobserved higher levels. The iterative self-consistent procedure described above was therefore repeated with the calculated distortion constants for $v=0$–50 obtained in each cycle being fitted to an NDE function of the form of Eq. (7)

TABLE VI. Parameters defining the recommended exponential near-dissociation expansions of Eq. (7) for the first five CDC's for the A state of I_2. The associated constants $K_7(v)$ are defined as $K_7(v)=0.0404\,K_6(v)/(v_D-v)^2$, while $v_D=55.570$ [see Eq. (10) and Table V]; the $X_m(5,C_5)$ constants have units cm^{-1}, while all the other parameters are dimensionless.

	$m=2$	$m=3$	$m=4$	$m=5$	$m=6$
$X_m(5,C_5)$	-9.99×10^{-6}	-1.15×10^{-7}	-3.47×10^{-9}	-1.41×10^{-10}	-6.68×10^{-12}
p_1^m	−0.793 274 32	−1.806 547 4	−1.694 953 5	−0.665 776 6	−0.790 637
p_2^m	0.180 523 92	0.687 924 9	0.522 639 7	−0.207 135 4	−0.245 756 9
p_3^m	$-2.954\,318\,5\times10^{-2}$	−0.147 125 59	−0.102 080 41	$8.893\,851\times10^{-2}$	0.105 747 43
p_4^m	$3.331\,406\,1\times10^{-3}$	$1.883\,931\,3\times10^{-2}$	$1.248\,379\,1\times10^{-2}$	$-1.493\,950\,8\times10^{-2}$	$-1.782\,239\,2\times10^{-2}$
p_5^m	$-2.603\,363\,0\times10^{-4}$	$-1.545\,768\,3\times10^{-3}$	$-9.936\,160\times10^{-4}$	$1.454\,199\,6\times10^{-3}$	$1.742\,104\,5\times10^{-3}$
p_6^m	$1.416\,658\,8\times10^{-5}$	$8.473\,351\times10^{-5}$	$5.306\,400\times10^{-5}$	$-9.089\,425\times10^{-5}$	$-1.093\,849\,9\times10^{-4}$
p_7^m	$-5.373\,197\times10^{-7}$	$-3.168\,339\,6\times10^{-6}$	$-1.931\,509\times10^{-6}$	$3.798\,039\times10^{-6}$	$4.591\,391\times10^{-6}$
p_8^m	$1.409\,765\times10^{-8}$	$8.102\,607\times10^{-8}$	$4.792\,00\times10^{-8}$	$-1.072\,390\times10^{-7}$	$-1.301\,889\times10^{-7}$
p_9^m	$-2.501\,58\times10^{-10}$	$-1.393\,192\times10^{-9}$	$-7.954\,83\times10^{-10}$	$2.019\,39\times10^{-9}$	$2.460\,76\times10^{-9}$
p_{10}^m	$2.859\,18\times10^{-12}$	$1.538\,71\times10^{-11}$	8.4352×10^{-12}	$-2.428\,1\times10^{-11}$	$-2.968\,2\times10^{-11}$
p_{11}^m	$-1.896\,5\times10^{-14}$	-9.854×10^{-14}	-5.156×10^{-14}	$1.684\,9\times10^{-13}$	2.065×10^{-13}
p_{12}^m	5.54×10^{-17}	2.78×10^{-16}	1.38×10^{-16}	-5.13×10^{-16}	-6.3×10^{-16}

TABLE VII. Molecular constants for levels of A state I_2, all in units cm^{-1}. Note that the associated values of O_v are defined by Eq. (10): $O_v = 0.0404\ N_v/(v_D - v)^2$.

v	$G(v)$	B_v	$D_v/10^{-9}$	$H_v/10^{-14}$	I_v	M_v	N_v
0	0.000	0.027 259 0	9.8945	−1.345	-4.62×10^{-20}	-1.82×10^{-25}	-8.77×10^{-31}
1	89.862	0.026 970 6	10.524	−1.662	-6.39×10^{-20}	-3.38×10^{-25}	-1.93×10^{-30}
2	176.633	0.026 671 6	11.336	−2.071	-8.67×10^{-20}	-4.89×10^{-25}	-3.09×10^{-30}
3	260.223	0.026 355 6	12.266	−2.566	-1.18×10^{-19}	-6.85×10^{-25}	-4.68×10^{-30}
4	340.540	0.026 021 4	13.309	−3.160	-1.61×10^{-19}	-9.97×10^{-25}	-7.35×10^{-30}
5	417.499	0.025 669 1	14.487	−3.884	-2.20×10^{-19}	-1.50×10^{-24}	-1.19×10^{-29}
6	491.025	0.025 298 2	15.831	−4.772	-2.97×10^{-19}	-2.24×10^{-24}	-1.90×10^{-29}
7	561.060	0.024 907 7	17.358	−5.849	-3.95×10^{-19}	-3.25×10^{-24}	-2.91×10^{-29}
8	627.562	0.024 497 1	19.071	−7.117	-5.09×10^{-19}	-4.45×10^{-24}	-4.16×10^{-29}
9	690.520	0.024 066 5	20.951	−8.547	-6.35×10^{-19}	-5.72×10^{-24}	-5.51×10^{-29}
10	749.952	0.023 617 4	22.955	−10.07	-7.63×10^{-19}	-6.93×10^{-24}	-6.82×10^{-29}
11	805.917	0.023 152 7	25.027	−11.61	-8.86×10^{-19}	-8.02×10^{-24}	-8.02×10^{-29}
12	858.515	0.022 676 2	27.100	−13.05	-9.98×10^{-19}	-9.02×10^{-24}	-9.15×10^{-29}
13	907.890	0.022 192 5	29.109	−14.34	-1.10×10^{-18}	-1.00×10^{-23}	-1.04×10^{-28}
14	954.221	0.021 706 2	31.002	−15.45	-1.19×10^{-18}	-1.11×10^{-23}	-1.18×10^{-28}
15	997.715	0.021 221 5	32.747	−16.39	-1.28×10^{-18}	-1.25×10^{-23}	-1.38×10^{-28}
16	1038.588	0.020 742 0	34.336	−17.23	-1.38×10^{-18}	-1.44×10^{-23}	-1.66×10^{-28}
17	1077.057	0.020 270 3	35.783	−18.06	-1.50×10^{-18}	-1.69×10^{-23}	-2.06×10^{-28}
18	1113.329	0.019 807 8	37.123	−18.97	-1.65×10^{-18}	-2.02×10^{-23}	-2.63×10^{-28}
19	1147.587	0.019 355 1	38.402	−20.06	-1.85×10^{-18}	-2.46×10^{-23}	-3.42×10^{-28}
20	1179.994	0.018 911 8	39.669	−21.42	-2.10×10^{-18}	-3.03×10^{-23}	-4.53×10^{-28}
21	1210.690	0.018 476 9	40.978	−23.12	-2.43×10^{-18}	-3.76×10^{-23}	-6.05×10^{-28}
22	1239.790	0.018 048 9	42.374	−25.25	-2.85×10^{-18}	-4.71×10^{-23}	-8.12×10^{-28}
23	1267.393	0.017 626 3	43.901	−27.86	-3.38×10^{-18}	-5.91×10^{-23}	-1.09×10^{-27}
24	1293.579	0.017 207 5	45.593	−31.03	-4.05×10^{-18}	-7.44×10^{-23}	-1.47×10^{-27}
25	1318.415	0.016 790 8	47.483	−34.80	-4.89×10^{-18}	-9.42×10^{-23}	-1.99×10^{-27}
26	1341.957	0.016 374 8	49.598	−39.26	-5.94×10^{-18}	-1.20×10^{-22}	-2.70×10^{-27}
27	1364.250	0.015 958 1	51.966	−44.48	-7.24×10^{-18}	-1.54×10^{-22}	-3.70×10^{-27}
28	1385.331	0.015 539 3	54.618	−50.59	-8.86×10^{-18}	-1.99×10^{-22}	-5.13×10^{-27}
29	1405.234	0.015 117 3	57.591	−57.75	-1.09×10^{-17}	-2.62×10^{-22}	-7.22×10^{-27}
30	1423.984	0.014 690 6	60.928	−66.21	-1.35×10^{-17}	-3.48×10^{-22}	-1.03×10^{-26}
31	1441.604	0.014 258 0	64.683	−76.33	-1.67×10^{-17}	-4.70×10^{-22}	-1.50×10^{-26}
32	1458.115	0.013 818 1	68.922	−88.56	-2.10×10^{-17}	-6.43×10^{-22}	-2.23×10^{-26}
33	1473.533	0.013 370 3	73.723	−103.5	-2.66×10^{-17}	-8.92×10^{-22}	-3.38×10^{-26}
34	1487.877	0.012 914 2	79.173	−122.0	-3.41×10^{-17}	-1.25×10^{-21}	-5.21×10^{-26}
35	1501.164	0.012 450 6	85.374	−145.1	-4.44×10^{-17}	-1.79×10^{-21}	-8.19×10^{-26}
36	1513.41	0.011 982	92.44	−174.	-5.84×10^{-17}	-2.59×10^{-21}	-1.31×10^{-25}
37	1524.64	0.011 511	100.5	−210.	-7.81×10^{-17}	-3.82×10^{-21}	-2.16×10^{-25}
38	1534.87	0.011 045	109.7	−256.	-1.06×10^{-16}	-5.76×10^{-21}	-3.64×10^{-25}
39	1544.12	0.010 589	120.2	−313.	-1.46×10^{-16}	-8.89×10^{-21}	-6.35×10^{-25}
40	1552.43	0.010 153	132.1	−386.	-2.05×10^{-16}	-1.42×10^{-20}	-1.15×10^{-24}
41	1559.82	0.009 747	145.9	−481.	-2.94×10^{-16}	-2.34×10^{-20}	-2.19×10^{-24}
42	1566.34	0.009 379	161.9	−608.	-4.33×10^{-16}	-4.03×10^{-20}	-4.40×10^{-24}
43	1572.00	0.009 058	180.5	−781.	-6.57×10^{-16}	-7.28×10^{-20}	-9.37×10^{-24}
44	1576.87	0.008 788	202.6	−1030.	-1.04×10^{-15}	-1.39×10^{-19}	-2.14×10^{-23}
45	1580.98	0.008 57	229.4	−1403.	-1.71×10^{-15}	-2.81×10^{-19}	-5.28×10^{-23}
46	1584.39	0.008 39	262.6	−1986.	-3.00×10^{-15}	-6.08×10^{-19}	-1.43×10^{-22}
47	1587.15	0.008 23	304.7	−2937.	-5.62×10^{-15}	-1.44×10^{-18}	-4.29×10^{-22}
48	1589.32	0.008 04	359.9	−4554.	-1.14×10^{-14}	-3.79×10^{-18}	-1.49×10^{-21}
49	1590.96	0.007 76	435.2	−7412.	-2.56×10^{-14}	-1.16×10^{-17}	-6.31×10^{-21}
50	1592.15	0.007 27	543.3	−12730.	-6.48×10^{-14}	-4.44×10^{-17}	-3.51×10^{-20}

before being used in the subsequent step. Since the v dependence of these constants is very drastic, with the values of particular $K_m(v)$ coefficients ranging over many orders of magnitude, one must be careful in choosing the weights associated with each of the input data. The present work used a scheme introduced by Tromp and Le Roy,[39] which set the uncertainty associated with each calculated $K_m(v)$ value as the lesser of 1% of its value or $\delta K_m(v) = \delta E/[J_{\max}(J_{\max}+1)]^m$, where δE is the average experimental error associated with the data set in question, and $J_{\max} = J_{\max}(v)$ is the highest J value associated with the data for that A-state v level.

For various $m_{\max}$ values and different types of models, the quality of fit to our 9552 assigned transition frequencies is summarized in Table IV. The results in column 4, where only directly calculated distortion constants are used, illustrate the slow convergence of the expansion in $[J(J+1)-\Omega^2]$ (see also Fig. 2). The results in the last col-

TABLE VIII. Molecular constants for A state I_2 (in cm^{-1} and Å); these T_e values neglect contributions from $Y_{0,0}$ terms.

			Present work	
	Ashby[a]	Viswanathan *et al.*[b]	Dunham	NDE[c]
T_e	10 906(±3)	10 906.8(±0.9)	10 907.416(±0.009)	10 907.436
T_0	10 845(±2)	10 846.6	10 846.389	10 846.387
D_e	1 641(±3)	1 640.2(±0.9)	1 639.938	1 639.918
D_0	1 595(±2)	1 593.3	1 593.854	1 593.856
ω_e	92.5 (±0.5)	94.95(±0.82)	92.946(±0.016)	92.870
$\omega_e x_e$	1.20 (±0.08)	2.43(±0.26)	1.565(±0.012)	1.484
B_e	0.028 17	0.028 45	0.027 398(±0.000 002)	0.027 405
α_e	0.000 547	0.000 420 2	0.000 275(±0.000 002)	0.000 297
R_e	3.071	3.056(±0.01)	3.1140	3.1136

[a]Vibrational constants from Ref. 24 and rotational constants from Ref. 23.
[b]Reference 27.
[c]Recommended values; based on the NDE parameterization of Table V.

umn, on the other hand, illustrate the efficacy of using Eq. (10), with its one additional empirical parameter, to accelerate convergence of the rotational expansion. The poor quality of the Dunham fits with constrained numerical CDC's (column 3) reflects the poor convergence and instability of this approach, as discussed in Sec. III B. Note too that the empirical Dunham fit of column 2 had 47 free parameters, while the NDE fits of columns 4 and 5, respectively, had only 25 and 26 free parameters. Although there is very little difference between the quality of fit for the last entries in column 5, and both involve the same number of free parameters, the case $m_{\max}=7$ is is preferred because it is expected to give more reliable predictions for very high J.

The form of Eq. (7) shows that plots of $\ln[K_m(v)/K_m^{\infty}(v)]$ vs v should approach zero as $v \to v_D$. The solid curves in Fig. 5 illustrate the fact that our NDE fits to the calculated distortion constants for $v=0$–50 explicitly incorporate this behavior. In contrast, the empirical Dunham expansions of Sec. III A (dashed and dotted curves) behave very badly at high v. The symbols in Fig. 5 represent the directly calculated values of these constants on the range spanned by the experimental data. The similarity in the form of the solid curves for the higher values of m provides further evidence for the validity of the approximate relation of Eq. (10).

The constants defining our final recommended global representation for the vibration rotation level energies of the $A\,^3\Pi_{1u}$ state of I_2 are listed in Tables V and VI. The vibrational energies are given by an [8/2] rational polynomial NDE where the leading expansion terms are quadratic in (v_D-v), and the rotational and centrifugal distortion constants by 12-term exponential NDE's of the form of Eq. (7). The rotational expansion is truncated at $m_{\max}=7$, with the $K_7(v)$ distortion constants being defined through Eq. (10) by the $K_6(v)$ NDE expansion of Table VI and the empirical parameter k_7 of Table V. The fact that the fitted value of k_7 is similar in magnitude to the ratios X_m/X_{m-1} for large m (see Table VI) is further evidence of the validity of using Eq. (10) to empirically represent additional higher-order centrifugal distortion terms. The Λ-doubling energy is represented by the same simple two-term Dunham-type expansion introduced in Eq. (2): $\pm[Q_{0,1}+Q_{1,1}(v+\frac{1}{2})][J(J+1)-1]$. To facilitate use of these results in making practical predictions, Table VII lists values of the vibrational energies and rotational constants implied by our expansions for $v=0$–50. The associated values of some conventional molecular constants are compared to the present Dunham results and to previously published values in Table VIII.

The resulting NDE expansions accurately represent the input data set, and ignoring perturbations and fine structure splittings, should provide realistic predictions for *all* unobserved higher bound and quasibound vibration–rotation levels of this state. The use of NDE functions makes this assertion valid even though the highest one third of the vibrational levels supported by this potential are not observed. Since the NDE expansion parameters have no physical significance, no uncertainties are listed for them. However, for all listed parameters, the number of digits quoted was chosen to ensure that predictions made with these constants would reproduce the input data to with a fraction of the experimental uncertainty. For the $G(v)$ and B_v constants in Table V, parameter rounding was based simply on the Watson criterion,[30] which requires that on average their net effect on predictions of the fitted data be less than 0.1 times the standard error of the fit. However, the expansion coefficients for the distortion constants were further rounded in an iterative manner which removes insignificant digits without loss of precision.[39,59] Computer file listings of these molecular constants, of subroutines for generating the associated NDE functions, and of the 9552 member data set may be obtained by electronic mail by sending a request to leroy@UWaterloo.ca or bernath@UWaterloo.ca, or by anonymous *ftp* from directory *pub/leroy/I2A* on our computer *theochem.uwaterloo.ca*.[43]

IV. DISCUSSION AND CONCLUSIONS

Two questions which may be raised regarding the above analysis concern the possible effect of inhomogeneous perturbations, and the validity of the assumed $n=5$ limiting behavior of Eq. (9). It is well known (see Fig. 1) that the

$A'\ ^3\Pi_{2u}$ state lies near and below the $A\ ^3\Pi_{1u}$ state of interest here, and theory tells us that these two states may be mixed by a rotational perturbation.[60] To search for these perturbations, we examined the series of (calc.–obs.) differences for all J's associated with each A-state vibrational level. When the residuals were based on band-by-band fits, no systematic behavior was observed, but many of those based on the global representation of Tables V and VI tended to show modest systematic trends which we attributed to weak global perturbations by the A' state. In addition, a well-defined local perturbation due to a level crossing was observed at $J=77$ in bands with $v_A=32$; it can be attributed to $v=43$ of the A' state,[5] and yielded a maximum deviation of approximately 0.04 cm^{-1}. Although calculations indicate that neighboring vibrational levels should also be locally perturbed by other A'-state levels, surprisingly, no further local perturbations were detected. This was taken as being due to the lack of data and to the low signal-to-noise ratio of the spectrum in this region.

As for most electronic states of I_2, the long-range potential for the $A\ ^3\Pi_{1u}$ state consists of the sum of terms

$$V(R)=D-C_5/R^5-C_6/R^6-C_8/R^8-C_{10}/R^{10}-\cdots . \tag{11}$$

For the $A\ ^3\Pi_{1u}$ state, the C_5 coefficient is very small in magnitude compared to those for many other electronic states of I_2, and its contribution to the long-range potential is much smaller than that associated with the next longest-range term, for which Saute and Aubert-Frécon[57] have predicted $C_6=2.01\times10^6$ cm^{-1} Å^6. Indeed, out to a distance of over 30 Å, where the total interaction is only ca. 0.01 cm^{-1}, the former is weaker than the latter. This might make it tempting to set the power of n appearing in Eqs. (5)–(9) at $n=6$ in the above NDE treatment. However, systematic tests showed that this approach had no advantages in compactness or quality of fit to the analysis based on $n=5$, and also had surprisingly little effect on the fitted value of v_D. This probably reflects the small difference between the powers 10/3 and 3 associated with $K_0^\infty(v)$ for these two cases, as well as the overall robustness of NDE representations.

In conclusion, some 9552 lines comprising some 79 vibrational bands of the $A-X$ spectrum of I_2 have been assigned and analysed. While a conventional double Dunham expansion is able to adequately represent these data, the higher-order distortion constants so obtained are demonstrably unreliable, and the resulting expression have essentially no predictive ability for vibrational or rotational levels beyond the range of the input data. In contrast, self-consistent fits based on the use of ''mechanically consistent'' calculated centrifugal distortion constants, with near-dissociation expansions being used to represent the vibrational energies and all rotational constants, yield an equally good fit to the data and should provide realistic predictions for all unobserved higher vibrational and rotational levels.

[1] R. S. Mulliken, Phys. Rev. **36**, 699 (1930).
[2] R. S. Mulliken, J. Chem. Phys. **55**, 288 (1971).
[3] J. A. Coxon, in *Molecular Spectroscopy*, Vol. 1, edited by R. F. Barrow, D. A. Long, and D. J. Millen (Specialist Periodical Report of the Chemical Society of London, 1973), p. 177.
[4] S. Gerstenkorn and P. Luc, J. Phys. **46**, 867 (1985).
[5] J. B. Koffend, A. M. Sibai, and R. Bacis, J. Phys. **43**, 1639 (1982).
[6] J. Tellinghuisen, J. Chem. Phys. **58**, 2821 (1971).
[7] J. Tellinghuisen, Chem. Phys. Lett. **49**, 485 (1977).
[8] J. Tellinghuisen, J. Chem. Phys. **78**, 2374 (1982).
[9] J. Tellinghuisen, J. Mol. Spectrosc. **94**, 231 (1982).
[10] X. Zheng, S. Fei, M. C. Heaven, and J. Tellinghuisen, J. Chem. Phys. **96**, 4877 (1992).
[11] S. Gerstenkorn and P. Luc, *Atlas du Spectre d'Absorption de la Molecule d'Iode, Vol. I. 14,800–20,000 cm^{-1}* (Laboratoire Aimé Cotton, CNRS II, Orsay, 1977).
[12] S. Gerstenkorn and P. Luc, *Atlas du Spectre d'Absorption de la Molecule d'Iode, Vol. II. 14,000–15,600 cm^{-1}* (Laboratoire Aimé Cotton, CNRS II, Orsay, 1978).
[13] S. Gerstenkorn, J. Vergès, and J. Chevillard, *Atlas du Spectre d'Absorption de la Molecule d'Iode, Vol. III. 11,000–14,000 cm^{-1}* (Laboratoire Aimé Cotton, CNRS II, Orsay, 1982).
[14] S. Gerstenkorn and P. Luc, *Atlas du Spectre d'Absorption de la Molecule d'Iode, Vol. IV. 19,700–20,035 cm^{-1}* (Laboratoire Aimé Cotton, CNRS II, Orsay, 1983).
[15] S. Gerstenkorn, P. Luc, and J. Vergès, *Atlas du Spectre d'Absorption de la Molecule d'Iode, Vol. O. 7,220–11,200 cm^{-1}* (Laboratoire Aimé Cotton, CNRS II, Orsay, 1993).
[16] Copies of all volumes of the Atlas may be obtained from the Laboratoire Aimé Cotton, Bâtiment 505, Campus d'Orsay, 91405 Orsay Cedex, France.
[17] R. D. Verma, J. Chem. Phys. **32**, 738 (1960).
[18] D. H. Rank and M. W. Baldwin, J. Chem. Phys. **19**, 1210 (1951).
[19] D. H. Rank and B. S. Rao, J. Mol. Spectrosc. **13**, 34 (1964).
[20] R. J. Le Roy, J. Chem. Phys. **52**, 2683 (1970).
[21] F. Martin, R. Bacis, S. Churassy, and J. Vergès, J. Mol. Spectrosc. **116**, 71 (1986).
[22] W. G. Brown, Phys. Rev. **38**, 1187 (1931).
[23] R. A. Ashby, Can. J. Phys. **57**, 698 (1979).
[24] R. A. Ashby and C. W. Johnson, J. Mol. Spectrosc. **84**, 41 (1980).
[25] S. Gerstenkorn, P. Luc, and J. Vergès, J. Phys. B **14**, L193 (1981).
[26] X. Zheng, S. Fei, M. C. Heaven, and J. Tellinghuisen, J. Mol. Spectrosc. **149**, 399 (1991).
[27] K. S. Viswanathan, A. Sur, and J. Tellinghuisen, J. Mol. Spectrosc. **86**, 393 (1981).
[28] J. Connes, H. Delouis, P. Connes, G. Guelachvili, J. P. Maillard, and G. Michel, Nouv. Rev. Opt. Appl. **1**, 3 (1970).
[29] This $K_m(v)$ notation simplifies the discussion and obviates the artificial sign difference associated with the conventional definition of $D_v=-K_2(v)$.
[30] J. K. G. Watson, J. Mol. Spectrosc. **66**, 500 (1977).
[31] J. L. Dunham, Phys. Rev. **41**, 721 (1932).
[32] S. Z. Moody and C. L. Beckel, Int. J. Quantum Chem. **IIIS**, 469 (1970).
[33] D. L. Albritton, W. J. Harrop, A. L. Schmeltekopf, and R. N. Zare, J. Mol. Spectrosc. **46**, 25 (1973).
[34] J. Tellinghuisen, Chem. Phys. Lett. **18**, 544 (1973).
[35] J. D. Brown, G. Burns, and R. J. Le Roy, Can. J. Phys. **51**, 1664 (1973).
[36] J. Hutson, J. Phys. B **14**, 851 (1981).
[37] D. L. Albritton, W. J. Harrop, A. L. Schmeltekopf, and R. N. Zare, J. Mol. Spectrosc. **46**, 89 (1973).
[38] J. M. Hutson, S. Gerstenkorn, P. Luc, and J. Sinzelle, J. Mol. Spectrosc. **96**, 266 (1982).
[39] J. W. Tromp and R. J. Le Roy, J. Mol. Spectrosc. **109**, 352 (1985).
[40] J. Tellinghuisen, J. Mol. Spectrosc. **44**, 194 (1972).
[41] R. J. Le Roy, *RKR1: A Computer Program Implementing the First-Order RKR Method for Determining Diatom Potential Energy Curves from Spectroscopic Constants* (University of Waterloo Chemical Physics Research Report CP-425, 1993).
[42] A copy of this program and associated documentation may be obtained by sending a request by electronic mail to leroy@UWaterloo.ca, or by anonymous *ftp* (see Ref. 43) from our computer theochem.uwaterloo.ca.
[43] To obtain this material by anonymous *ftp*, begin by using the command *ftp* theochem.uwaterloo.ca to connect to our computer. The response to the userid prompt should be *anonymous* and that to the password prompt should be the caller's e-mail address. The specified subdirectory may then

be accessed with the command cd pub/leroy/subdirectory_name, and the desired files copied with the command get file-name.
[44] J. Tellinghuisen, J. Mol. Spectrosc. **122**, 455 (1987).
[45] R. J. Le Roy, *LEVEL 6.0: A Computer Program for Solving the Radial Schrödinger Equation for Bound and Quasibound Levels and Calculating Various Expectation Values and Matrix Elements* (University of Waterloo Chemical Physics Research Report CP-555, 1995).
[46] R. J. Le Roy and R. B. Bernstein, J. Chem. Phys. **52**, 3869 (1970).
[47] R. J. Le Roy, Can. J. Phys. **50**, 953 (1971).
[48] R. J. Le Roy, in *Molecular Spectroscopy*, Vol. 1, edited by R. F. Barrow, D. A. Long and D. J. Millen (Specialist Periodical Report of the Chemical Society of London, 1973), p. 113.
[49] J. W. Tromp and R. J. Le Roy, Can. J. Phys. **60**, 26 (1982).
[50] R. J. Le Roy, J. Chem. Phys. **73**, 6003 (1980).
[51] R. J. Le Roy (unpublished).
[52] R. J. Le Roy and R. B. Bernstein, Chem. Phys. Lett. **5**, 42 (1970).
[53] R. J. Le Roy and M. G. Barwell, Can. J. Phys. **53**, 1983 (1975).
[54] R. J. Le Roy, in *Semiclassical Methods in Molecular Scattering and Spectroscopy*, edited by M. S. Child (Reidel, Dordrecht, 1980), p. 109.
[55] J. K. Knipp, Phys. Rev. **53**, 734 (1938).
[56] T. Y. Chang, Rev. Mod. Phys. **39**, 911 (1967).
[57] M. Saute and M. Aubert-Frécon, J. Chem. Phys. **77**, 5639 (1982).
[58] M. D. Davies, J. C. Shelley, and R. J. Le Roy, J. Chem. Phys. **94**, 3479 (1991).
[59] J. Tellinghuisen, J. Mol. Spectrosc. **137**, 248 (1989).
[60] H. Lefebvre-Brion and R. W. Field, *Perturbations in the Spectra of Diatomic Molecules* (Academic, New York, 1986).